

Storing images in warm atomic vapor

M. Shuker,¹ O. Firstenberg,¹ R. Pugatch,² A. Ron,¹ and N. Davidson²

¹*Department of Physics, Technion-Israel Institute of Technology, Haifa 32000, Israel*

²*Department of Physics of Complex Systems, Weizmann Institute of Science, Rehovot 76100, Israel*

versus an optical storage system. It is a promising approach to store information in warm atomic vapor for up to μs without loss of transparency. Both the intensity and phase patterns of the optical information are stored in the atomic medium. The storage duration is limited by the atomic diffusion. A technique to reduce the effect of atomic diffusion is presented.

PACS numbers: 42.50.Gy, 32.70.Jz

When a resonant light pulse ("probe") impinges upon a gas of atoms, it is strongly absorbed, exciting the atoms to an upper state. However, if a second "pump" beam is present, which couples a second state to the same excited state, then the "probe" pulse will be able to pass the sample - a phenomenon known as electromagnetically induced transparency (EIT) [1]. The unique properties of EIT allow for a wide range of coherent light-matter phenomena, including non-linear optics [2], entanglement [3], generation of quantum pulses of light [4], and quantum communication [5]. In Ref. [6], the group velocity of the probe pulse, in a medium of ultra-cold atoms, was decreased to 17 m/s and similar results were achieved in warm vapor [7]. In Refs. [8, 9, 10], it was demonstrated that the probe pulse can be completely stopped, while it is contained inside the medium, by shutting off the pump. The pulse can be recovered by reopening the pump beam after a certain "storage duration". A prominent feature of this technique is the reversible and coherent storage of the information carried by the probe, in the atomic coherences.

Here, we report a method for reversibly capturing complex three-dimensional light fields using EIT in atomic vapor [1, 8]. The storage experiments discussed above have utilized a transverse Gaussian mode for both pump and probe beams. The current research is focused on slowing and storing information imprinted in the transverse plane of the probe beam ("images"), and on reducing the effects of atomic diffusion. In a previous work [11], the ability to slow images and delay them for several ns was demonstrated, using dispersion from far-detuned absorption lines. In the current work, we use EIT to slow images to a group velocity of several thousands m/s, achieving delays of several μs . We further use the unique properties of EIT to store the images in the atomic medium for a similar duration. The long slowing delays and storage durations are comparable with the typical diffusion time in which atoms cross the image. We demonstrate the deteriorating effect of diffusion by storing images of digits for different durations. Finally, we introduce a technique to diminish the effect of

atomic diffusion by alternating the phase of neighboring features. This technique, which is the atomic analogue of the optical phase-shift lithography [12], is demonstrated by storing an image of three lines and studying the effect of flipping the phase of adjacent lines.

Slowing of images may prove useful for various image processing and image-correlation applications. An intriguing possibility is to use the diffusion during slowing or storage as a complex diffusion filter, thus realizing an all optical edge detector [13]. In the context of quantum information processing, a single-cell device for multi-qubit memory can be implemented, e.g., by a spatial array of optical qubits in the transverse plane. Storing images, rather than slowing them, has the fundamental advantages of supporting longer delays and completely converting the optical information to atomic coherence, hence making it more amenable to various methods of manipulation, e.g., phase conjugation [14].

The storage experiments were performed within the D1 transition of ^{87}Rb [10] as depicted in Fig. 1.a. Two Zeeman sub-levels of the ground state ($|F=2; m_F=0\rangle, |F=2; m_F=+2\rangle$) are used as the two lower levels of a Λ -system. The experimental setup is depicted in Fig. 1.b. An external cavity diode laser (ECDL) is stabilized to the $F=2 \rightarrow F'=1$ transition. The laser is divided into two beams of perpendicular polarizations, the pump and the probe, using a polarizing beam-splitter (PBS). The pump and the probe pass through acousto-optic modulators (AOM), allowing us to precisely control the Raman detuning. The pump beam is shaped as a large Gaussian beam with a waist radius of $w_{\text{pump}} = 2.1$ mm and a total intensity of 5.8 mW. The probe beam is shaped as a Gaussian beam with a waist radius of $w_{\text{probe}} = 1$ mm and intensity of 200 μW and passes through a binary image mask, which is a standard resolution target. The plane of the image-mask is imaged onto the center of the vapor cell using two lenses (the optical design and the feature size of the images insure that the diffraction along the cell's length is negligible). The pump and the probe are recombined on a second PBS and co-propagate towards the cell. A quar-

ter wave-plate before the cell converts the pump and the probe polarizations to σ^+ and σ^- respectively. We use a 5 cm long vapor cell, containing isotopically pure ^{87}Rb and 10 Torr of Neon buffer gas. Frequent collisions with the buffer gas induce Dicke-like narrowing [15], increasing the acceptance angle of the probe beam [16, 17], thus allowing for smaller features in the transverse plane. The diffusion coefficient of Rb atoms is determined from independent measurements to be $D = 10\text{cm}^2/\text{s}$. The temperature of the cell is $\sim 52^\circ\text{C}$, providing a Rubidium vapor density of $\sim 1.3 \times 10^{11}/\text{cc}$. The cell is placed within a four-layered magnetic shield, and a set of Helmholtz coils provides a small, $B_z = 50\text{mG}$, axial magnetic field to set the quantization axis.

The experimental sequence of the storage experiments is detailed in Fig. 1.c. A pulse of the probe beam (Gaussian; $\sigma=5\mu\text{s}$) travelled in the EIT medium with a group velocity of $\sim 8000\text{m/s}$ — resulting in a *slowly propagating image* [11]. The images were stored in the medium by turning off the pump after about half of the probe pulse had exit the cell. After an arbitrary storage duration, the pump beam was turned on, and the stored image reappeared. Upon exiting the cell, the beams were separated using polarization optics, and the probe beam was imaged onto a CCD camera, whose focus was adjusted to the exit plane of the cell. The camera trigger was set to measure only the restored part of the probe beam (see Fig. 1.c), and special care is taken to avoid the detection of the leaked part of the probe. As a proof-of-principle, we stored images of the digits '2', '6', and '9' in the atomic vapor. The images were created using a standard resolution target as a mask, and by shifting the mask to imprint different digits in different measurements. Fig. 2 shows the images without slowing (left column), with slowing only (center column) and after being stored and retrieved (right column). Evidently, the image of the digit '2', which was slowed for $6\mu\text{s}$, was smoothed, and its sharp edges were softened (similar images were achieved for the other digits). We attribute this effect to atomic diffusion during the slow propagation of the dark-state polariton [18]. The diffusion effect is pronounced due to the sharp and narrow features in the image and due to the significantly larger delay time, compared with a previous demonstration of slow images in hot vapor [11]. The lower signal-to-noise ratio in the slowed image is mainly due to the lower transmission, compared with the off-resonance image.

The images of the digits '2', '6', and '9' were stored for 2, 6, and $9\mu\text{s}$, respectively. During the storage, the images are encoded in the quantum state of the atomic ensemble [8] and thus susceptible to degradation through various relaxation processes, such as spin-exchange, collisions, and diffusion. Nevertheless, the main features survive through the storage process, and the digits are still identifiable. Two degradation effects are evident from the stored images: broadening of the image features due

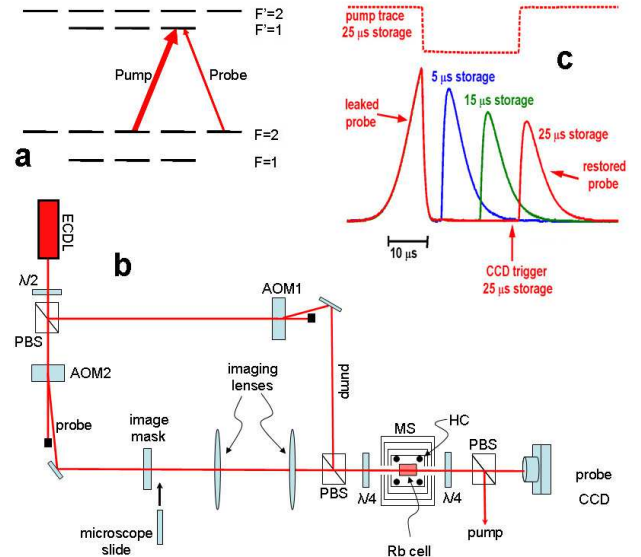


FIG. 1. Experimental setup and pulse sequence. (a) Energy level diagram showing the $F=1$ and $F=2$ states of ^{87}Rb . The Pump beam is shown as a red arrow from $F=1$ to $F=2$, and the Probe beam is shown as a red arrow from $F=2$ to $F=1$. (b) Schematic of the experimental setup. A red laser beam passes through an EOM, a $\lambda/2$ waveplate, and a PBS. It then passes through AOM2, an image mask, and imaging lenses. The beam is reflected by a microscope slide and passes through a lens, a PBS, and a $\lambda/4$ waveplate. It then enters the Rb cell, which is surrounded by a magnetic shield (MS) and Helmholtz coils (HC). The beam is reflected by a PBS and a $\lambda/4$ waveplate, and then passes through a lens and a PBS. The probe beam is detected by a CCD camera. The pump beam is reflected by a PBS and a $\lambda/4$ waveplate, and then passes through a lens and a PBS. The pump beam is detected by a CCD camera. (c) Pulse sequence showing the probe pulse (5 μs), storage durations (5, 15, 25 μs), and the restored probe pulse. The probe pulse is shown as a red arrow, and the storage durations are shown as blue, green, and red arrows. The restored probe pulse is shown as a red arrow. The pump trace is shown as a red dashed line, and the CCD trigger is shown as a red dashed line.

to diffusion and decreased signal-to-noise ratio due to various decay mechanisms and technical limitations. In order to study quantitatively the limiting factors of the spatial resolution, we stored an image of three resolution lines. Both the lines' thickness and spacing were $340\mu\text{m}$ at the center of the cell. The left side of Fig. 3 shows the experimental results for storage durations of 2, 10, 20, and $30\mu\text{s}$ (left column) as well as the theoretical prediction (right column). For storage time of $2\mu\text{s}$, the lines are clearly visible, and, as storage time increases to $30\mu\text{s}$, the image blurs and its visibility diminishes. The theoretical prediction is based on the assumption that, for a plane-wave pump, the storage of a weak probe field effectively maps its envelope, $E(\mathbf{r}, 0)$, onto the spatially-dependent slowly-varying ground-state coherence, $\sigma_{bc}(\mathbf{r}, 0)$ [8]. Assuming that the internal state of each individual atom does not change as a result of diffusion, we find that the motion of the atoms during storage can be effectively described by adding a classical diffusion term, $D\nabla^2\sigma_{bc}$, to the Bloch equation, where D is the spatial diffusion coef-

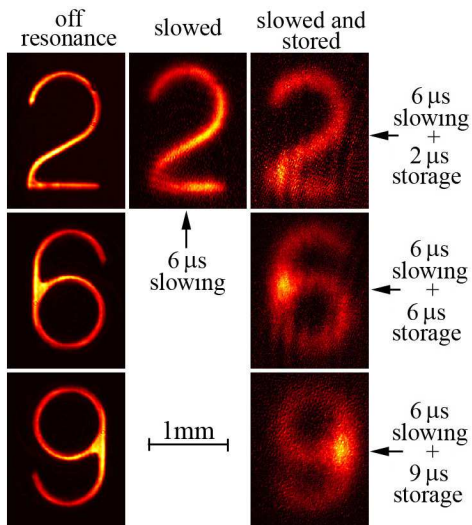


FIG. 1. A series of images showing the storage and retrieval of probe fields in warm vapor. The images show the evolution of the probe field from an off-resonance state to a slowed state and finally to a stored state. The storage durations are 2, 6, and 9 μs . The images show the evolution of the probe field from an off-resonance state to a slowed state and finally to a stored state. The storage durations are 2, 6, and 9 μs . The images show the evolution of the probe field from an off-resonance state to a slowed state and finally to a stored state. The storage durations are 2, 6, and 9 μs .

efficient [19]. The ensemble average of the different atoms arriving to the same small macroscopic volume determines the retrieved probe field [20]. Therefore, retrieved fields after storage durations t and $t + \tau$ are related by:

$$|E(\mathbf{r}, t + \tau)|^2 = \left| e^{-\frac{\Gamma}{2}\tau} \int d^3\tilde{\mathbf{r}} |E(\tilde{\mathbf{r}}, t)| e^{i\phi(\tilde{\mathbf{r}}, t)} G_\tau(\mathbf{r} - \tilde{\mathbf{r}}) \right|^2, \quad (1)$$

where $G_\tau(\mathbf{r}) = (2\pi D\tau)^{-3/2} \exp[-|\mathbf{r}|^2 / (4D\tau)]$ is the three-dimensional diffusion propagator, Γ is the ground-state decay rate, $E(\tilde{\mathbf{r}}, t) = |E(\tilde{\mathbf{r}}, t)| e^{i\phi(\tilde{\mathbf{r}}, t)}$, and $\phi(\tilde{\mathbf{r}}, t)$ is the phase pattern. Eventually, the initial conditions for the calculation in Fig. 3 are $|E(\tilde{\mathbf{r}}, t = 2\mu\text{s})|$, obtained by taking the *square-root* of the measured intensity image after storage of 2 μs . We used $\phi(\tilde{\mathbf{r}}, t) = 0$ for the constant-phase experiments and an appropriate phase pattern for experiments where the phase of different areas was shifted (see below).

The diffusion of atoms during the storage is evidently the main limit on the storage and retrieval resolution in a medium of warm atoms. A possible method to increase the spatial resolution is based on the fact that the phase pattern of the light field is stored on top of its intensity distribution. By appropriately manipulating the phase of different points in the image, the immunity to diffusion can be improved. In the field of photolithography, a well established technique to reduce the effect of spreading

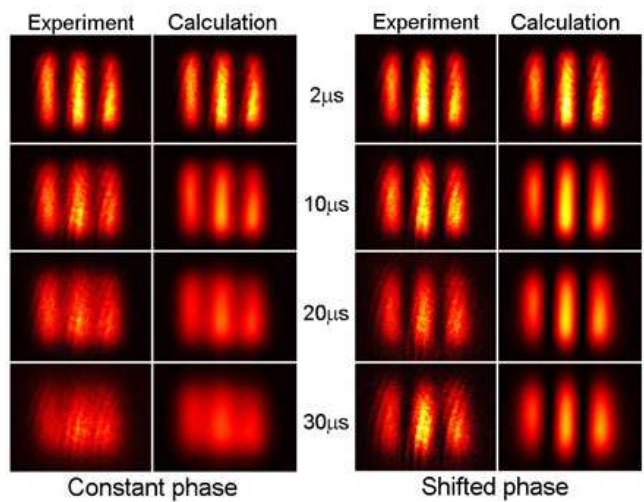


FIG. 3. Comparison of experimental results with calculations for different storage durations up to 30 μs . The images show the evolution of the probe field from an off-resonance state to a slowed state and finally to a stored state. The storage durations are 2, 10, 20, and 30 μs . The images show the evolution of the probe field from an off-resonance state to a slowed state and finally to a stored state. The storage durations are 2, 10, 20, and 30 μs .

due to diffraction is the so-called phase-shift lithography [12]. Its concept is based on flipping the phases of neighboring features of the image, so that light diffracting to the areas between them will interfere destructively. We implemented an analogous technique in order to mitigate the effect of atomic diffusion. Using microscope slides, we shifted the phase of the two outer lines by $\sim \pi$ with respect to the central line in the probe image. Therefore, the ground-state coherence, created in the atomic medium, had opposite phases in neighboring lines. During storage, atoms of opposite phases diffused to the area between the lines, and the amplitude of the coherence field sum up to zero. Therefore, no probe beam was generated in the forward direction [21], keeping these areas dark in the restored image.

The results of the shifted-phase experiment as well as suitable calculations are depicted in the right side of Fig. 3. The calculation is performed by introducing an appropriate stepwise phase pattern. The dramatic effect of the phase-shift on the visibility of the stored features is pronounced — even after 30 μs , the lines are well separated, while the respective images in the constant-phase case are completely diffused. These results demonstrate that indeed a *complex field* is stored in the atomic medium. We have previously demonstrated the topological stability of stored optical vortices to diffusion [18]. The current method is a generalized technique that can be adapted to *arbitrary* images. Figure 4 shows the measured and calculated visibility of the stored image as a function of

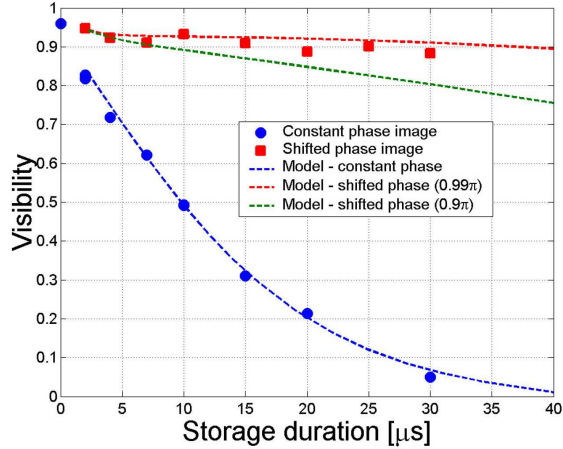


FIG. 1. Visibility of the stored image as a function of storage duration, t , for a constant phase image (blue circles) and a shifted phase image (red squares). The solid lines represent the theoretical model for the constant phase image (blue circles) and the shifted phase image (red squares). The dashed lines represent the experimental data for the constant phase image (blue circles) and the shifted phase image (red squares). The storage duration is in μs .

the storage duration. The rapid decrease of visibility in the constant phase experiment as well as the persistent high visibility in the shifted-phase experiment are well described by our theoretical model.

The phase-shift method can be applied in cases where there is either partial or full a-priori information about the image. In the demonstration above, a prior knowledge regarding the location of the lines in the image allowed us to construct a suitable phase mask. If complete information regarding the image is available, an elaborate phase mask can be designed, even for complicated images, to minimize the effects of diffusion [12]. If no a-priori information regarding the image is available, other techniques can be used to reduce the effect of diffusion. Increasing the buffer gas pressure is a straight-forward option, limited by the one and two-photon broadening mechanisms. In this case the phase pattern can be used to store information, which might be suitable for certain quantum memory realizations [22, 23]. Another novel method to reduce the effects of diffusion on arbitrary stored images, based on storing the *transform plane*, was recently investigated theoretically [24], and implemented experimentally [25].

In conclusion, we have demonstrated the ability to store images in warm atomic vapor. The main limitation of the spatial resolution is the diffusion of atoms

during the storage. A technique to reduce the effect of diffusion by alternating the phase in neighboring features of the image has been demonstrated by storing $340 \mu\text{m}$ thick lines for as long as $30 \mu\text{s}$, with negligible decrease in their visibility. Our experiment is a trivial case of storing a three-dimensional complex light field, where the shape in the longitudinal (temporal) direction is a simple Gaussian. In principle, it should be possible to store more elaborate temporal shapes, thus storing three dimensional information ("movie").

Helpful discussions with Paz London and Amit Ben-kish are acknowledged. This work was partially supported by the fund for encouragement of research in the Technion.

E. Harris, *Phys. Rev.* **50**, 100 (1941).
 E. Harris and J. H. Hau, *Phys. Rev. Lett.* **82**, 100 (1999).
 D. Ulanov and A. I. A. O. Ulanov, *Phys. Rev. Lett.* **84**, 100 (2000).
 D. E. S. and C. R. S. A. An. R. F. Assou, A. Z. rov, *Phys. Rev. Lett.* **93**, 100 (2004).
 Duan, D. Ulanov, J. I. Cra. an. Zo. r. atur **414**, 100 (2005).
 Hau, E. Harris, Z. Dutton, an. C. H. B. roo, atur **397**, 100 (2005).
 Kas. A. aut n ov, A. Z. rov, Ho. r. G. u. D. u. n. Y. Y. Z. v. IEEE, rans. at Ana. a. n. Int. **26**, 100 (2005).
 F. s. au. r. an. D. u. n. s. v. tt **84**, 100 (2005).
 C. u. Z. Dutton, C. H. B. roo, an. Hau, atur **409**, 100 (2005).
 D. F. ps. A. F. s. au. r. A. ar. a. swort, an. D. u. n. s. v. tt **86**, 100 (2005).
 Ca. a. o. C. J. Broa. nt. I. A. K. an. an. J. C. How, s. v. tt **98**, 100 (2005).
 D. v. nson, s. s. o. a. **46**, 100 (2005).
 G. G. oa. o. n. an. Y. Y. Z. v. IEEE, rans. at Ana. a. n. Int. **26**, 100 (2005).
 A. Z. rov, A. B. ats. o. Ko. a. rovs. a. a. Y. ostovts. v. G. an. u. s. v. tt **88**, 100 (2005).
 Frst n. r. u. r. A. B. n. K. s. D. Fr. n. Dav. son, an. A. on. s. v. A. **76**, 100 (2005).
 C. Bo. art. D. osto. ar. an. t. s. v. A. **71**, 100 (2005).
 u. r. Frst n. r. u. at. A. B. n. K. s. A. on. an. Dav. son, s. v. A. **76**, 100 (2005).
 u. at. u. r. Frst n. r. A. on. an. Dav. son, s. v. tt **98**, 100 (2005).
 Frst n. r. u. r. u. at. D. Fr. n. Dav. son, an. A. on. s. v. A. **77**, 100 (2005).
 Y. X. ao. I. ov. ova. D. F. ps. an. a. swort, s. v. tt **96**, 100 (2005).

an Zao Jan an F Y n s i v
 A 77 / ' //
 F s au r an D u n s i v A 65
 / //
 D u n v o o s 75 / ' //

Zao an Y X ao an F Y n s i v
 A 77 / ' //
 K u as tu Ca a o an J C How s
 v tt 100 / ' //